HHS Public Access

Author manuscript

Aerosol Sci Technol. Author manuscript; available in PMC 2016 February 18.

Published in final edited form as:

Aerosol Sci Technol. 2013 ; 47(4): 435–443. doi:10.1080/02786826.2012.762757.

Design and Evaluation of a Personal Diffusion Battery

Donna J. H. Vosburgh[a], **Timothy Klein**[b], **Maura Sheehan**[c], **T. Renee Anthony**[d], and **Thomas M. Peters**[d]

[a]Department of Occupational and Environmental Safety and Health , University of Wisconsin-Whitewater , Whitewater , Wisconsin , USA

[b]TAK Ind., LLC , Muskegon , Michigan , USA

[c]Department of Health , West Chester University , West Chester , Pennsylvania , USA

[d]Department of Occupational and Environmental Health , The University of Iowa , Iowa City , Iowa , USA

Abstract

A four-stage personal diffusion battery (pDB) was designed and constructed to measure submicron particle size distributions. The pDB consisted of a screen-type diffusion battery, solenoid valve system, and electronic controller. A data inversion spreadsheet was created to solve for the number median diameter (NMD), geometric standard deviation (GSD), and particle number concentration of unimodal aerosols using stage number concentrations from the pDB combined with a handheld condensation particle counter (pDB+CPC). The inversion spreadsheet included particle entry losses, theoretical penetrations across screens, the detection efficiency of the CPC, and constraints so the spreadsheet solved to values within the pDB range. Size distribution parameters (NMD, GSD, and number concentration) measured with the pDB+CPC with inversion spreadsheet were within 25% of those measured with a scanning mobility particle sizer (SMPS) for 5 of 12 polydisperse combustion aerosols. For three tests conducted with propylene torch exhaust, the pDB+CPC with inversion spreadsheet successfully identified that the NMD was smaller than the constraint value of 16 nm. The ratio of the nanoparticle portion of the aerosol compared to the reference (R_{nano}) was calculated to determine the ability of pDB+CPC with inversion spreadsheet to measure the nanoparticle portion of the aerosols. The R_{nano} ranged from 0.87 to 1.01 when the inversion solved and from 0.06 to 2.01 when the inversion solved to a constraint. The pDB combined with CPC has limited use as a personal monitor but combining the pDB with a different detector would allow for the pDB to be used as a personal monitor.

INTRODUCTION

Airborne nanoparticles—particles with a diameter of at least one dimension smaller than 100 nm (ASTM Standard E2456 2006)—are present in many workplaces. Diffusion causes nanoparticles to have high rates of deposition in the human respiratory system, regardless of age or breathing pattern (Daigle et al. 2003; Kim and Jaques 2005). Toxicological studies have determined that, depending on their chemistry, crystalline structure, and activity,

Supplementary materials are available for this article.

nanoparticles may have increased toxicity compared to larger particles of the same composition (Johnston et al. 2000; Warheit et al. 2004, 2007; Karlsson et al. 2009).

Direct-reading instruments measuring particle number or surface area concentration can be sensitive indicators of airborne nanoparticles (Mohr et al. 2005), but portable direct-reading instruments that measure personal nanoparticle size distributions are unavailable. Nanoparticles agglomerate rapidly producing aerosols farther from a source to be composed of fewer, larger particles than were at the source. Depending on the worker's proximity to the source and to the direct-reading instrument, the worker's exposure may be different from the measured airborne nanoparticle concentration. Thus, a breathing zone measurement is needed. Some direct-reading instruments such as diffusion chargers and condensation particle counters (CPC) are small enough to be carried by a worker but do not provide concentrations by size for submicron particles (Baron and Willeke 2001).

A screen-type diffusion battery can be coupled with a low-cost, small, direct-reading instrument to obtain submicron size distribution information. In a screen-type diffusion battery, the aerosol is passed through a series of stages that hold screens (Sinclair and Hoopes 1975). Diffusion causes particles to collect on the screens and not be counted by the detector. The number concentration and particle size collected depend on screen characteristics (Cheng and Yeh 1980; Cheng et al. 1980; Yeh et al. 1982; Cheng et al. 1985). A mathematical data inversion algorithm is required to estimate the distribution of the original aerosol based on the theoretical particle penetrations of the screens, the detection efficiency of the detector compared to the reference instrument used, and particle losses of the aerosol entering the screen-type diffusion battery (Cheng and Yeh 1984). A data inversion technique using an iterative approach increases the accuracy of the aerosol distribution estimates (Twomey 1975). Such an approach was successfully implemented within a spreadsheet to process data from cascade impactors (O'Shaughnessy and Raabe 2003).

Screen-type diffusion batteries have the potential to be used in a personal nanoparticle direct-reading instrument if certain issues can be addressed. Screen-type diffusion batteries have traditionally had many stages and were coupled with large switching valves (Cheng and Yeh, 1984; Gorbunov et al. 2009). The combined size prohibited them from being used to collect personal measurements. Using only the minimum number of stages and reducing the size of the switching valve, a screen-type diffusion battery could be developed to assess personal nanoparticle exposures by determining the number median diameter (NMD), the geometric standard deviation (GSD), and the number concentration of a submicron aerosol.

In this study, a personal diffusion battery (pDB) was designed and evaluated for the purpose of determining the concentration of nanoparticles in a submicron aerosol. The pDB consisted of a four-stage screen-type diffusion battery and a solenoid valve system that automatically switched from one pDB stage to the next pDB stage, changing the path of the airflow through different numbers of screens in the pDB. To evaluate its potential use, the pDB was combined with a CPC (pDB+CPC) to record number concentrations for each pDB stage, and an inversion spreadsheet was created to estimate the aerosol NMD, GSD, and

number concentration. Future work to miniaturize a submicron aerosol detector would enable pDB+CPC combination to be used in personal sampling.

METHODS

Personal Diffusion Battery (pDB) Design

As shown in Figure 1a, the pDB consisted of a conductive sampling tube, four-stage screen-type diffusion battery, solenoid valve manifold system, and electronic controller. The weight of the pDB in the backpack, excluding the detector and electrical battery, was 3.2 kg (7 lbs). To allow aerosol from a worker's breathing zone to enter the screen-type diffusion battery, a 96-cm sampling tube was attached to the front of the screen-type diffusion battery. The diffusion battery was assembled from a series of 13, 25-mm conductive filter cassette pieces (225–329, SKC Inc., Eighty Four, PA, USA) with stages identified as Stage A through D (Figure 1b). Sets of stainless steel screens (Twill 635 US standard mesh, Dorstener Wire Tech, Spring, TX, USA) were installed at three locations in the diffusion battery (zero in Stage A; five in Stage B; 11 in Stage C; and 16 in Stage D). The screen fiber wire diameter was 0.02 mm, thickness was 0.04 mm, average weight was 0.0548 g, and density was 8000 kg m^{-3}. The calculated solid volume fraction of each screen was 0.349. The inside diameter of the cassettes was 21.1 mm. Each stage was fitted with a 5-mm plastic connector and tubing to that was connected to the solenoid valve manifold (SAM1614–4G2015, Gem Sensors & Controls, New Britain, CT, USA). An electronic controller was programmed to sequentially open the solenoid valves and divert airflow through the diffusion battery in a repeated sequence: Stage A; Stage B; Stage C; Stage D; Stage A; etc. (Figure 1b). The solenoid valves were attached to a common manifold that conveyed the aerosol to the detector.

For development of the pDB, a handheld CPC (Model 3007, TSI, Inc., Shoreview, MN, USA) was selected as the detector, and the coupled instrument was referred to as the pDB +CPC. This commercially available CPC was selected because it measures particle number concentration from 10 nm to approximately 1 μm and had the ability to compensate for changes in inlet pressure to maintain a constant airflow of 0.7 L min^{-3} (Matson et al. 2004). The 0.7 L min^{-1} flow rate of the CPC resulted in a superficial velocity of 0.03 m s^{-1}, within the laminar flow regime (Reynolds number = 46.4).

pDB Stage Penetration and Detection Efficiency

Use of the pDB+CPC required knowledge of penetration by particle size for each stage of the pDB and the detection efficiency of the CPC. The penetration of aerosol through Stage A and the 96 cm transport tube was determined experimentally as described in the online supplementary information (Measurement of Stage A Penetration). Detection efficiency by particle size d (DE_d) was determined experimentally as described in the online supplementary information (Determined DE_d Values from Monodispersed Results).

For Stage B, C, and D, theoretical penetration ($P_{n,d}$) by size was calculated as (Cheng and Yeh 1984):

$$P_{n,d}=10^{-nm} \quad (1)$$

where d is the particle diameter, n is the number of screens, and m is:

$$m_d=A_0Pe^{-2/3}+A_1R^2+A_2Pe^{-1/2}R^{2/3} \quad (2)$$

In Equation 2, Pe is the Peclet number, R is the interception, and parameters A_0, A_1, and A_2 are:

$$A_0=1.17\,B \quad (3)$$

$$A_1=0.434\,B/k \quad (4)$$

$$A_2=0.539\,B/(k^{1/2}) \quad (5)$$

where k is:

$$k=-0.5\,ln(2\alpha/\pi)+(2\alpha/\pi)-0.75-((2\alpha/\pi)^2)/4) \quad (6)$$

α is the screen solid volume fraction, B is:

$$B=4\alpha h/\pi(1-\alpha)D_f \quad (7)$$

where h is the screen thickness and D_f is the diffusion coefficient.

Development and Evaluation of an Inversion Spreadsheet for use with the pDB+CPC

A data inversion spreadsheet was developed to estimate the NMD, GSD, and number concentration of a lognormal, unimodal aerosol from particle number concentrations measured with the CPC after exiting the four stages of the pDB (N_A , N_B , N_C , and N_D). Following Cheng and Yeh (1984), the spreadsheet included theoretical screen penetrations for each stage, $P_{A,d}$, and DE_d . The inversion was implemented in an Excel spreadsheet (2007, Microsoft Corp.,Seattle, WA, USA) using the “Inversion Method” described by O’Shaughnessy and Raabe (2003). Constraints were input into the spreadsheet to require the spreadsheet to solve to values within the range of the pDB which were based on the theoretical stage penetrations. The initial constraints were an aerosol distribution number concentration greater than N_A, NMD between 1 and 500 nm, and GSD between 1.1 and 3. The “Solver” function was used to adjust the initial NMD, GSD, and number concentration until the sum of square differences between the total number concentrations that passed through each and the input number concentrations from the pDB+CPC was minimized. Details of implementation are described in the online supplementary information (Implementation of the Inversion Spreadsheet).

The inversion spreadsheet was theoretically evaluated to determine the lower and upper limits of the distribution NMD that could be determined given a minimum number of pDB stages. The inversion spreadsheet was used to process simulated particle size distributions (assumed NMD, GSD, and number concentration) using all four stages. A simulated NMD was considered smaller than the lower limit or larger than the upper limit if at least one of the four following occurred: the simulated distribution NMD was more than ±10% different from the original distribution NMD, the simulated distribution GSD was more than ±5% different from the original distribution GSD, the simulated distribution number concentration was more than ±5% different from the original distribution number concentration, and/or the simulated inversion solved to a constraint.

The inversion spreadsheet was then used to determine the minimum number of stages that could be used and still produce reasonable estimates of the original size distribution. The number of stages was unacceptable if at least one of the following occurred: the inversion distribution NMD was more than ±10% different from the original distribution NMD, the inversion distribution GSD was more than ±5% different from the original distribution GSD, the inversion distribution number concentration was more than ±5% different from the original distribution number concentration, and/or the inversion solved to a constraint.

Polydisperse Aerosols

The particle number concentration by size estimated by the pDB+CPC with inversion spreadsheet was compared to that measured with an SMPS for two test aerosols: exhaust from a propylene torch (Model MAP-Pro, Worthington Cylinders, Columbus, OH, USA) and a burning incense stick. Those aerosols were chosen to examine different size distributions. The propylene torch exhaust was composed of particles smaller than 100 nm and when fresh, could have a NMD smaller than the lower limit of the inversion spreadsheet. The incense was composed of particles both smaller and larger than 100 nm. As shown in Figure 2, the test aerosol was directed into a mixing chamber and diluted with HEPA filtered air. The test aerosol was passed into a sampling chamber where it was measured with the pDB+CPC and immediately after with the SMPS (SMPS+C model 5.4, Grimm, Ainring, Germany). A pump (Model Omni, BGI Incorporated, Walthan, MA, USA) was attached to the sampling chamber to keep a constant airflow through the chamber.

Two pDB solenoid valve timings were used for these tests: 60 s a stage for a total time of 240 s to cycle through the four stages; and 20 s a stage for a total time of 80 s to cycle through the four stages. The CPC was set to log particle number concentrations every second. The first ten 1-s measurements of each stage were not included in the stage mean to allow the previous aerosol to clear the pDB before measuring the next aerosol passing the stage. Three runs of alternating pDB+CPC measurements followed by SMPS measurements were conducted for each aerosol and timing.

The inversion spreadsheet was used to estimate the NMD, GSD, and number concentration of the test aerosol, using the mean of 1-s number concentrations measured by the CPC for each stage of the pDB+CPC (N_A , N_B , N_C , and N_D). The inversion constraints were the same as above except for the NMD constraints, which were ≥16 nm and ≤287 nm. The estimates of NMD, GSD, and number concentration from the pDB+CPC with inversion

were compared to those measured by the SMPS. Results were identified as acceptable if the NMD, GSD, and/or number concentration estimated with the pDB+CPC with inversion spreadsheet differed from the SMPS measured distribution by ±25%.

The ratio (R_{nano}) of number concentration of nanoparticles between 9.4 to 100 nm measured by the pDB+CPC with inversion spreadsheet (*pDB+CPC nanoparticles*) to number concentration of nanoparticles between 9.4 to 100 nm measured by the SMPS (*SMPS nanoparticles*) was calculated for each run using Equation (8).

$$R_{nano}=(pDB+CPC\ nanoparticle)/(SMPS\ nanoparticle) \quad (8)$$

RESULTS

The pDB+CPC Inversion Spreadsheet Limitations

The results of the original and simulated distributions identified as the lower and upper limits, along with the diameter below the lower limit and above the upper limit, are shown in Table 1. The lower and upper limits of the pDB+CPC with inversion spreadsheet were 17 and 286 nm, respectively. The simulated inversion distribution for the 16 nm original distribution solved to a constraint with regard to GSD for the original GSD of 1.4. The simulated inversion distribution for the 287 nm GSD of 1.4 original distribution solved to a GSD of 1.52, which was greater than the 5% difference allowed.

The results of the required stage number evaluation are shown in Table 2. The distribution used to represent the lower limit of the inversion was NMD of 17 nm, GSD of 1.4, and number concentration of 50,000 particles cm^{-3}. The distribution used to represent the upper limit of the inversion was NMD of 286, GSD of 1.4, and number concentration of 50,000 particles cm^{-3}. The combinations that solved for both distributions were: Stages A, B, and C; Stages A, B, and D; and the four stage combination.

Polydisperse Aerosols

The results of measuring exhaust from a propylene torch and burning incense are shown in Tables 3 and 4, Figures 3 and 4. The 240-s propylene torch distributions measured by the SMPS had a NMD of 15 nm (below the lower limit of the pDB+CPC with inversion spreadsheet) with GSD ranging from 1.42 to 1.49 (Table 3, Figure 3), while the 80-s distributions were slightly larger with a NMD of 17 nm and GSD ranging from 1.43 to 1.49. The number concentrations for the 240-s distributions were approximately 10,000 particles cm^{-3} less than the 80-s distributions. The NMD of the 240-s propylene torch distributions measured by the pDB+CPC with inversion spreadsheet all solved to 16 nm which was the alert that the NMD was below the lower limit of the pDB+CPC. Although the GSD values were within the acceptable criteria, the GSD ranged from 1.30 to 1.38, all less than the GSD values measured by the SMPS. The number concentrations measured by the pDB+CPC with inversion spreadsheet were also within the acceptable criteria. The pDB+CPC with inversion spreadsheet met the acceptable requirements for all NMDs, GSDs, and number concentrations when measuring the propylene torch exhaust using the 80-s timing. The *R*

$_{nano}$ for propylene torch exhaust (Table 4) ranged from 0.90 to 1.08 for the 240-s results, which all solved to an NMD constraint, and ranged from 0.87 to 0.93 for the 80-s results.

The 240-s incense distributions measured by the SMPS had a NMD of 97 to 107 nm with a GSD ranging from 1.74 to 1.82 (Table 3, Figure 4) while the 80-s distributions were slightly narrower with a NMD of 97 nm and a GSD ranging from 1.57 to 1.74. The number concentrations of the 240-s distributions were greater than the 80-s distributions. The NMD of the 240-s incense distributions measured by the pDB+CPC with inversion spreadsheet ranged from 87 to 156 nm and 69 to 113 nm for the 80-s distributions. Two of the three 240-s and two of the three 80-s distributions solved to the constraint GSD = 1.3. Three of the incense runs were greater than the ±25% criteria for NMD and two were greater than ±25% for GSD and one was greater than ±25% for number concentration. All of the incense runs that were greater than ±25% for NMD, GSD, and number concentration had solved to a constraint. Although the last 80-s incense run solved to a constraint, the NMD, GSD, and number concentration estimate were all within the ±25% acceptable criteria. The R_{nano} for the incense exhaust (Table 4) was 1.01 and 0.91 for the two measurements that did not solve to a constraint. R_{nano} ranged from 0.06 to 2.01 for the measurements runs where the pDB +CPC inversion solved to a constraint.

DISCUSSION

A pDB that can be placed in a backpack to be carried by a worker was designed and constructed. When combined with a handheld CPC, the pDB+CPC with inversion spreadsheet was used to determine differences between submicron distributions. The NMD of polydisperse aerosols measured with the pDB+CPC with inversion spreadsheet was within 2 nm for the propylene torch when it did not solve to a constraint and within 50 nm for incense even with four of the six incense measurements solving to a constraint (Table 3). The spreadsheet indicated when the distribution NMD was smaller than 16 nm, which was the case for the propylene torch exhaust aerosol.

The pDB+CPC with inversion spreadsheet was used to determine the nanoparticle component of the polydisperse aerosols with a high level of accuracy compared to the SMPS. For results where the pDB+CPC with inversion spreadsheet did not solve to a constraint, the R_{nano} value ranged from 0.87–1.01 (Table 4). Differences in the number concentration caused by the NMD below the limit of the pDB+CPC with inversion spreadsheet did not have a large effect on R_{nano} due to the distribution falling below 100 nm. A substantial difference was seen for the incense R_{nano} results. The incense aerosol was less stable than the propylene torch exhaust (Figure 4). Consequently, the pDB+CPC with inversion spreadsheet solved to a constraint for most tests. Differences in NMD and GSD from the pDB+CPC inversion solving to a constraint caused a substantial amount of the number concentration to fall above or below the 100 nm cut off. But by solving to a constraint, the calculated nanoparticle component of the distribution was flagged for the operator of the pDB+CPC with inversion spreadsheet. Shortening the valve timing from 240 to 80 s did not substantially affect the ability of the pDB+CPC with inversion spreadsheet to measure particle size distribution. There was only one 80-s run where the pDB+CPC estimated NMD was more than 25% different from the SMPS measurement while there

were three 240-s runs where the NMD was more than 25% different (Table 3). This study only looked at the two timings and future work is needed to determine the minimum timing for the pDB+CPC. Even with the 80-s measurement, the pDB+CPC was almost five times faster than the six-minute measurement time required for a full scan of the SMPS used in this study.

To allow the pDB to fit in a backpack, the design of the pDB was different than screen-type diffusion battery set-ups used in past studies. However, that did not limit the success of the pDB+CPC with inversion spreadsheet. The superficial velocity of the screens in the pDB screen-type diffusion battery was two-thirds that of the lowest superficial velocity of past studies, after correcting for differences in atmospheric pressure (Cheng and Yeh 1980; Cheng et al. 1980; Yeh et al. 1982; Cheng et al. 1985). The theoretical penetrations of the screen-type diffusion battery were successfully put into the inversion even though the superficial velocity was lower than those in past studies. The entire airflow in the pDB was directed through the screen-type diffusion battery and through a 90° turn before going into the solenoid valve manifold. In past studies, the majority of the airflow went straight through the screen-type diffusion battery with only a fraction of the airflow turned 90° to go into the detector (Cheng and Yeh 1980; Cheng et al. 1980; Yeh et al. 1982; Cheng et al. 1985). The differences in airflow through the pDB versus past studies appears to have been successfully addressed by using $P_{A,d}$ in the inversion.

The inversion created for the pDB+CPC had two important differences from the program used by Cheng and Yeh (1984) for their screen-type diffusion battery. The first difference was that the inversion for the pDB+CPC was created in a commonly used software program and could be recreated without knowledge of computer programming. The second difference is that the pDB+CPC inversion used the theoretical screen penetrations for the entire size distribution and constrained the inversion by including a lower and upper NMD limit. Cheng and Yeh (1984) used a size selection device before their screen-type diffusion battery to create a maximum penetration particle diameter. With the maximum penetration particle diameter, their inversion program included only penetration values equal to 1 for particle diameters larger than the maximum penetration particle diameter. Programming the penetration values to equal 1 while not identifying an upper limit for their inversion, did not allow any way for the operator of the pDB+CPC with inversion spreadsheet to be alerted if the distribution NMD was larger than the upper limit of the inversion but below the particle diameter of maximum penetration. No lower limit of the inversion was determined. The pDB+CPC inversion had penetration values for particle diameters up to 1000 nm and a lower and upper NMD limit. As shown by the propylene torch results (Table 3) if the NMD falls below the lower limit of the pDB+CPC with inversion spreadsheet the operator of the pDB+CPC with inversion spreadsheet is alerted. If a NMD distribution included particles larger than the upper limit of the inversion spreadsheet but smaller than the upper limit of the CPC (1000 nm), the pDB+CPC with inversion spreadsheet should solve to the NMD upper constraint of 286 nm. However, this was not verified in this study.

There are situations under which the pDB+CPC was not theoretically or laboratory tested. The pDB+CPC was designed for unimodal aerosols and was not tested with multi-modal aerosols. Most likely the inversion would solve to a constraint but that is unknown. Also, the

pDB+CPC was not challenged with significantly larger particles often found in work environments, such as respirable particles. Particles larger than 1000 nm should not be measured by the pDB+CPC but it is unknown if they would interrupt the function of the pDB if the larger particles built up on the screen surfaces. Using only three stages of the pDB could reduce the size of the pDB even more. Future work is needed to verify that using the two sets of three stages identified (Table 2) will accurately measure polydisperse aerosols.

The pDB was designed to be carried in a backpack by a worker thus causing minimal interference with the worker's tasks. However, tilting the TSI CPC 3007 can cause the optics to flood with condensation fluid (TSI Incorporated 2004) which restricts the use of the pDB+CPC for use as an area monitor or to measure personal exposures by placing a sampling tube in a worker's breathing zone. A miniaturized electrical classifier (Li et al. 2009) was recently developed in efforts to enable personal measurement of nanoparticle size distributions but also relies on a CPC 3007 for particle detection. Future work is needed to identify a robust detector that can be used in a backpack with the pDB and other miniaturized particle size classifiers.

CONCLUSIONS

A four-stage pDB was designed to be coupled with a direct-reading instrument to measure the size distributions of submicron aerosols. A data inversion spreadsheet was developed to convert the CPC number concentration of each pDB stage to a size distribution estimate to provide additional information on unimodal submicron aerosols containing nanoparticles. In a theoretical evaluation, the pDB+CPC inversion was found capable of determining the particle size distribution of an aerosol with a NMD between 17 to 286 nm with all four pDB stages.

Experiments were conducted and the NMD measured with the pDB+CPC with inversion spreadsheet was within 2 nm of that measured with a SMPS for propylene torch exhaust and within 50 nm for incense. The R_{nano} of number concentration between 9.4 to 100 nm measured by the pDB+CPC with inversion spreadsheet to that measured by the SMPS was from 0.87 to 1.01 when the inversion did not solve to a constraint and from 0.06 to 2.01 when the inversion did solve to a constraint. Future work is needed to challenge the pDB with larger aerosols, find a detector that can be placed in a backpack, and experimentally verify the upper limit of the inversion.

Supplementary Material

Refer to Web version on PubMed Central for supplementary material.

Acknowledgments

Funding for this project was provided by a NIOSH Heartland Center for Occupational Health and Safety Grant (T42OH008491) and NIOSH K01 grant (OH009255). The authors would like to thank Dr. Patrick O'Shaughnessy for his help with the inversion spreadsheet.

References

ASTM Standard E2456. Standard Terminology Relating to Nanotechnology. PA: West Conshohocken: ASTM International; 2006. www.astm.org

Baron, PA.; Willeke, K. Aerosol Measurement: Principles, Techniques and Applications. 2. New York: John Wiley and Sons, Inc; 2001.

Cheng YS, Keating JA, Kanapilly GM. Theory and Calibration of a Screen-Type Diffusion Battery. J Aerosol Sci. 1980; 11:549–556.

Cheng YS, Yeh HC. Theory of a Screen-Type Diffusion Battery. J Aerosol Sci. 1980; 11:313–320.

Cheng YS, Yeh HC. Analysis of Screen Diffusion Battery Data. Am Ind Hyg Assoc J. 1984; 45:556–561.

Cheng YS, Yeh HC, Brinsko KJ. Use of Wire Screens as a Fan Model Filter. Aerosol Sci Technol. 1985; 4:165–174.

Daigle CC, Chalupa DC, Gibb FR, Morrow PE, Oberdörster G, Utell MJ. Ultrafine Particle Deposition in Humans During Rest and Exercise. Inhal Toxicol. 2003; 15:539–552. [PubMed: 12692730]

Gorbunov B, Priest ND, Muir RB, Jackson PR, Gnewuch H. A Novel Size-Selective Airborne Particle Size Fractionating Instrument for Health Risk Evaluation. Ann Occup Hyg. 2009; 53:225–237. [PubMed: 19279163]

Johnston CJ, Finkelstein JN, Mercer P, Corson N, Gelein R, Oberdörster G. Pulmonary Effects Induced by Ultrafine PTFE Particles. Toxicol Appl Pharmacol. 2000; 168:208–215. [PubMed: 11042093]

Karlsson HL, Gustafsson J, Cronholm P, Möller L. Size-Dependent Toxicity of Metal Oxide Particles—A Comparison Between Nano-and Micrometer Size. Toxicol Lett. 2009; 188:112–118. [PubMed: 19446243]

Kim CS, Jaques PA. Total Lung Deposition of Ultrafine Particles in Elderly subjects during controlled breathing. Inhal Toxicol. 2005; 17:387–399. [PubMed: 16020035]

Li L, Chen DR, Qi C, Kulkarni PS. A Miniature Disk Electrostatic Aerosol Classifier (mini-disk EAC) for Personal Nanoparticle Sizers. J Aerosol Sci. 2009; 40:982–992.

Matson U, Ekberg LE, Afshari A. Measurement of Ultrafine Particles: A Comparison of Two Handheld Condensation Particle Counters. Aerosol Sci Technol. 2004; 38:487–495.

Mohr M, Lehmann U, Rutter J. Comparison of Mass-Based and Non-Mass-Based Particle Measurement Systems for Ultra-Low Emissions from Automotive Sources. Environ Sci Technol. 2005; 39:2229–2238. [PubMed: 15871258]

O'Shaughnessy PT, Raabe OG. A Comparison of Cascade Impactor Data Reduction Methods. Aerosol Sci Technol. 2003; 37:187–200.

Sinclair D, Hoopes GS. A Novel form of Diffusion Battery. Am Ind Hyg Assoc J. 1975; 36:39–42. [PubMed: 1111266]

Incorporated, TSI. Model 3007 Condensation Particle Counter Operation and Service Manual. Shoreview, MN: TSI Incorporated; 2004.

Twomey S. Comparison of Constrained Linear Inversion and an Iterative Nonlinear Algorithm Applied to the Indirect Estimation of Particle Size Distributions. J Comput Phys. 1975; 18:188–200.

Warheit DB, Laurence BR, Reed KL, Roach DH, Reynolds GA, Webb TR. Comparative Pulmonary Toxicity Assessment of Single-Walled Carbon Nanotubes in Rats. Toxicol Sci. 2004; 77:117–125. [PubMed: 14514968]

Warheit DB, Webb TR, Reed KL, Frerichs S, Sayes CM. Pulmonary Toxicity Study in Rats with Three forms of Ultrafine-TiO_2 Particles: Differential Responses Related to Surface Properties. Toxicology. 2007; 230:90–104. [PubMed: 17196727]

Yeh HC, Cheng YS, Orman MM. Evaluation of Various Types of Wire Screens as Diffusion Battery Cells. J Colloid Interface Sci. 1982; 86:12–16.

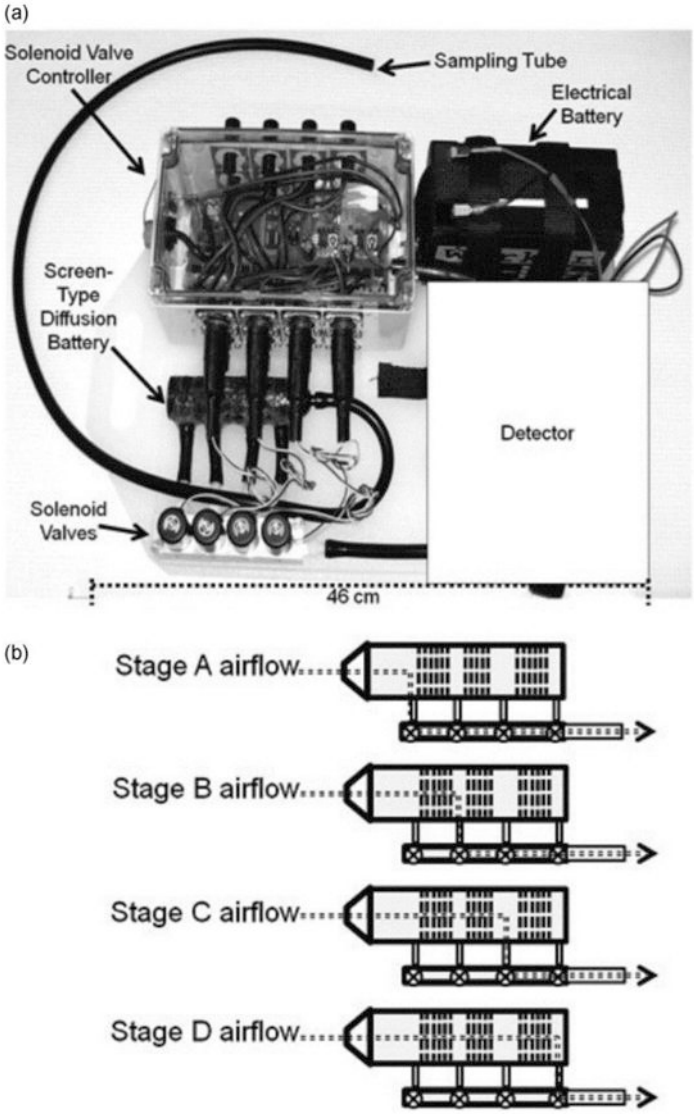

FIG. 1.

(a) Personal diffusion battery (pDB) that can be placed in a backpack. (b) Airflow through each stage of pDB.

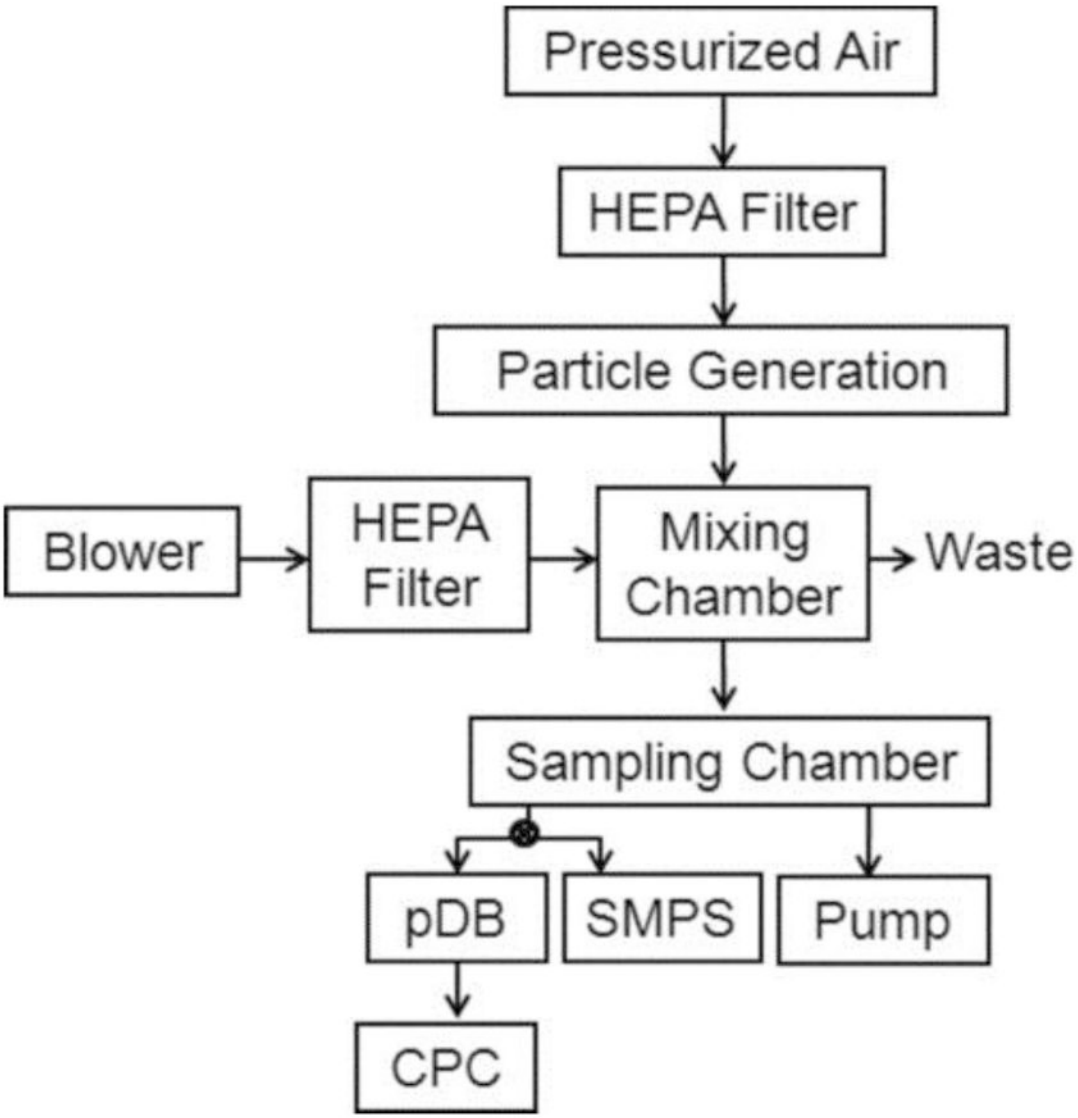

FIG. 2.
Experimental set up to test the pDB+CPC with inversion spreadsheet using combustion aerosols.

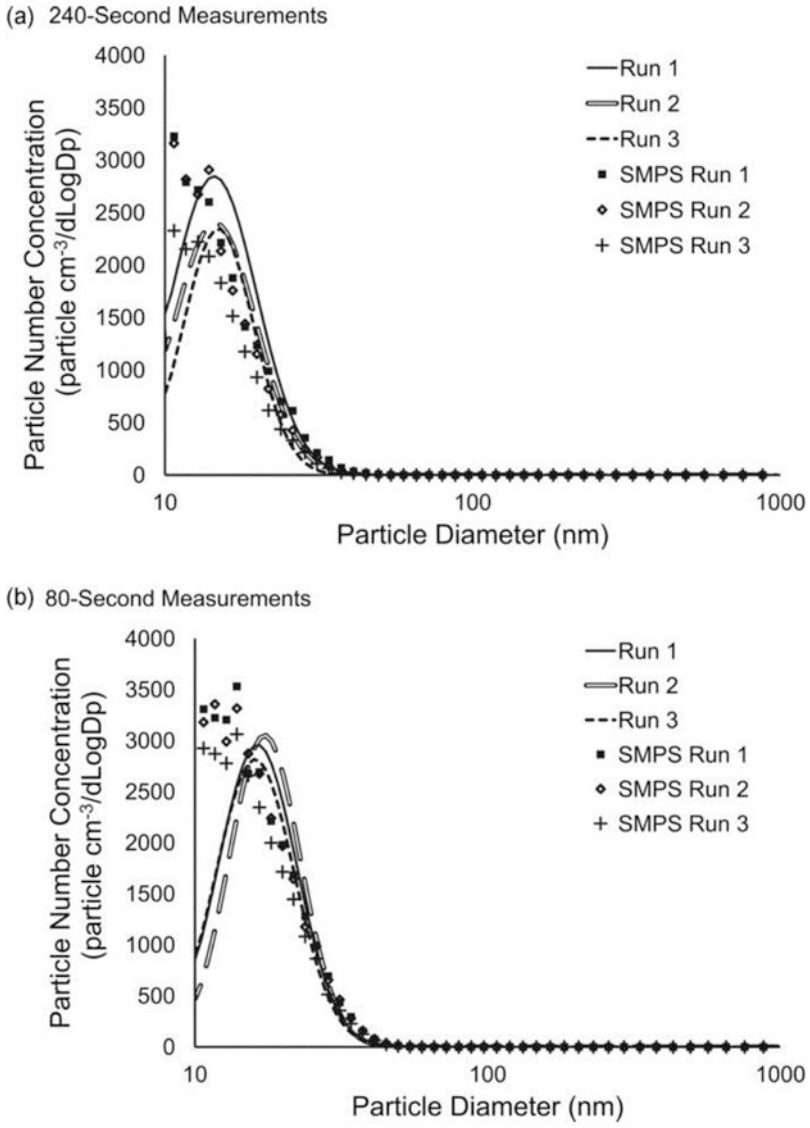

FIG. 3.

Comparison of the three propylene torch runs measured by the SMPS and the pDB+CPC with inversion spreadsheet for the (a) 240-s measurements and (b) 80-s measurements.

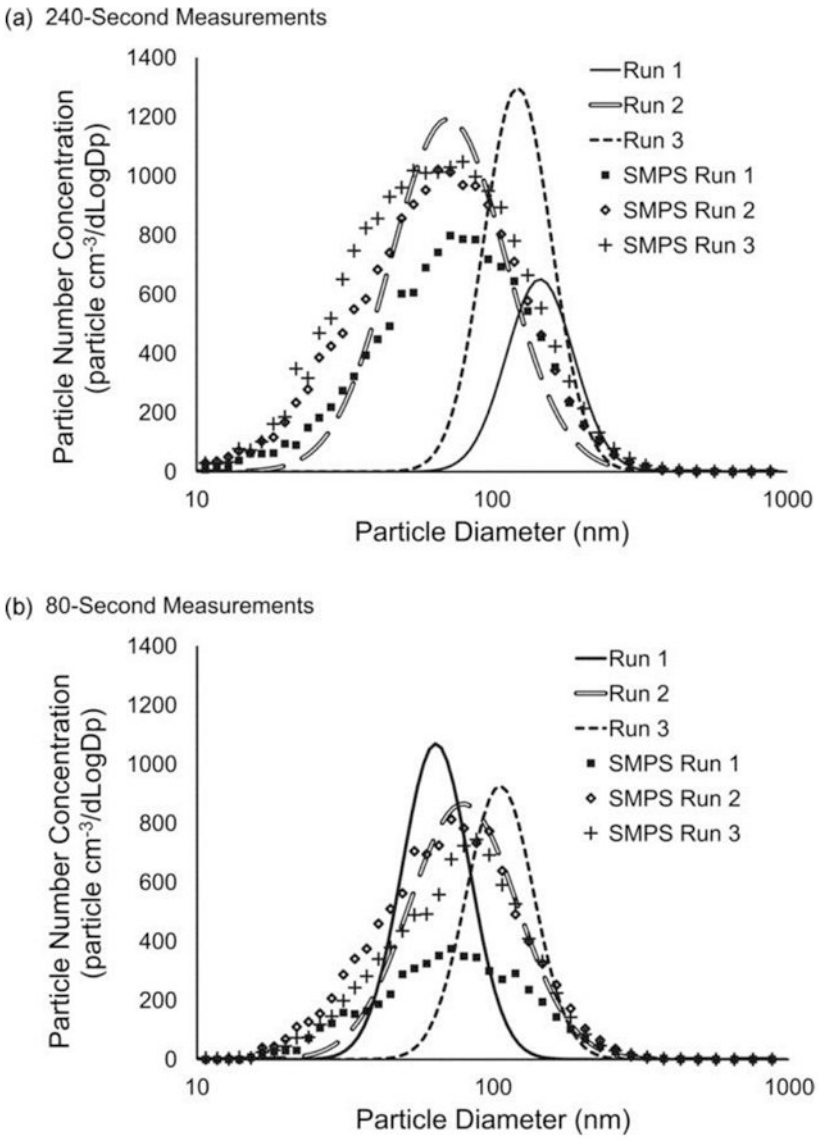

FIG. 4.

Comparison of the three incense runs measured by the SMPS and the pDB+CPC with inversion spreadsheet for the (a) 240-s measurements and (b) 80-s measurements.

TABLE 1

Original distributions and simulated inversion distribution results for the lower and upper NMD that could be distinguished with the pDB+CPC inversion and the results for the distributions with NMD below the lower limit and above the upper limit

Original distribution			Inversion distribution		
NMD (nm)	**GSD**	**Number concentration (particle cm^{-3})**	**NMD (nm)**	**GSD**	**Number concentration (particle cm^{-3})**
16	1.40	50,000	17	1.3[a,b]	47,489
16	2.00	50,000	16	2.00	49,982
16	2.80	50,000	16	2.80	50,003
17	1.40	50,000	17	1.40	49,997
17	2.00	50,000	17	2.00	49,993
17	2.80	50,000	17	2.80	50,010
286	1.40	50,000	287	1.41	50,010
286	2.00	50,000	281	1.98	49,755
286	2.80	50,000	286	2.80	49,987
287	1.40	50,000	310	1.52[b]	50,343
287	2.00	50,000	282	2.00	49,726
287	2.80	50,000	285	2.79	49,851

[a] Represents inversion results that solved to a constraint.

[b] Represents inversion results when one of the following occurred: the inversion distribution NMD was more than ±10% different from the original distribution NMD, the inversion distribution GSD was more than ±5% different from the original distribution GSD, or the inversion distribution number concentration was more than ±5% different from the original distribution number concentration.

TABLE 2

Inversion distribution results for varying number of pDB+CPC stages to determine minimum number of stages required for the NMD particle size range of 17–286 nm

	Lower limit distribution NMD = 17 nm, GSD = 1.4 number concentration = 50,000			Upper limit distribution NMD = 286 nm, GSD = 1.4 number concentration = 50,000		
Data inversion stages	**NMD (nm)**	**GSD**	**Number concentration (particle cm^{-3})**	**NMD (nm)**	**GSD**	**Number concentration (particle cm^{-3})**
A,B	18	1.3[b]	48,241	272	1.3[a,b]	49,847
B,C	500[a,b]	3.0[a,b]	38,092[b]	304[b]	1.50[b]	50,251
C,D	500[a,b]	3.0[a,b]	38,092[b]	273	1.3[a,b]	49,837
A,C	18	1.3[a,b]	47,912	272	1.3[a,b]	49,852
B,D	500[a,b]	3.0[a,b]	38,092[b]	303[b]	1.49[b]	50,247
A,D	19[b]	1.3[a,b]	47,675	272	1.3[a,b]	49,857
A,B,C[c]	17	1.40	49,996	278	1.34	49,910
B,C,D	500[a,b]	3.0[a,b]	38,092[b]	273	1.3[a,b]	49,847
A,C,D	18	1.31[b]	47,947	272	1.3[a,b]	49,852
A,B,D[c]	17	1.40	49,998	281	1.36	49,940
A,B,C,D[c]	17	1.40	49,997	287	1.41	50,010

[a] Represents inversion results that solved to a constraint.

[b] Represents inversion results where at least one of the following occurred: the inversion distribution NMD was ±10% different from the original distribution NMD, the inversion distribution GSD was ±5% different from the original distribution GSD, or the inversion distribution number concentration was ±5% different from the original distribution number concentration.

[c] Indicates distributions where all parameters were met.

TABLE 3

Polydisperse aerosol distributions measured with the SMPS and pDB+CPC with inversion spreadsheet. The total number concentration is reported here

		SMPS measured			pDB+CPC with inversion spreadsheet		
Aerosol	**Timing (s)**	**NMD (nm)**	**GSD**	**Number concentration (particle cm^{-3})**	**NMD (nm)**	**GSD**	**Number concentration (particle cm^{-3})**
Propylene torch	240	15	1.49	31,378	16[a]	1.38	33,898
Propylene torch	240	15	1.42	29,302	16[a]	1.36	27,544
Propylene torch	240	15	1.42	21,187	16[a]	1.30	23,457
Incense	240	107	1.75	96,022	156[b]	1.3[a, b]	64,160[b]
Incense	240	97	1.74	114,793	87	1.56	103,647
Incense	240	97	1.82	131,896	131[b]	1.3[a,b]	107,312
Propylene torch	80	17	1.43	43,633	18	1.30	37,782
Propylene torch	80	17	1.49	42,725	19	1.32	37,618
Propylene torch	80	17	1.43	37,955	18	1.36	35,945
Incense	80	97	1.57	56,766	69[b]	1.3[a]	46,220
Incense	80	97	1.74	82,325	95	1.52	77,969
Incense	80	97	1.57	72,589	113	1.3[a]	66,139

[a] Represents inversion results that solved to a constraint.

[b] Represents inversion results when one of the following occurred: the pDB+CPC with inversion spreadsheet distribution NMD was ±25% different from the SMPS measured distribution NMD, the pDB +CPC with inversion spreadsheet distribution GSD was ±25% different from the SMPS measured distribution GSD, the pDB+CPC with inversion spreadsheet distribution number concentration was ±25% different from the SMPS measured distribution number concentration.

TABLE 4

Nanoparticle number concentrations measured with the pDB+CPC with inversion spreadsheet and the SMPS

Aerosol	Timing (s)	pDB+CPC nanoparticle (particle cm^{-3})	SMPS nanoparticle (particle cm^{-3})	R_{nano}
Propylene torch	240	32,286	31,378	1.03[a]
Propylene torch	240	26,417	29,302	0.90[a]
Propylene torch	240	22,950	21,187	1.08[a]
Incense	240	2,720	46,348	0.06[a,b]
Incense	240	63,873	63,487	1.01
Incense	240	15,471	70,144	0.22[a,b]
Propylene torch	80	37,766	43,633	0.87
Propylene torch	80	37,623	42,725	0.88
Propylene torch	80	35,229	37,955	0.93
Incense	80	42,463	21,115	2.01[a,b]
Incense	80	42,400	46,499	0.91
Incense	80	20,213	38,574	0.52[a]

[a] Represents inversion results that solved to a constraint.

[b] Represents inversion results when one of the following occurred: the pDB+CPC with inversion spreadsheet distribution NMD was ±25% different from the SMPS measured distribution NMD, the pDB+CPC with inversion spreadsheet distribution GSD was ±25% different from the SMPS measured distribution GSD, the pDB+CPC with inversion spreadsheet distribution number concentration was ±25% different from the SMPS measured distribution number concentration.